J Mater Sci (2011) 46:5559–5567
DOI 10.1007/s10853-011-5506-8

ECAP processing and mechanical milling of Mg and Mg–Ti powders: a comparative study

Gülhan Çakmak · Tayfur Öztürk

Received: 21 February 2011 / Accepted: 23 March 2011 / Published online: 7 April 2011

Abstract A study was carried out into the possibility of employing ECAP processing in lieu of mechanical milling for the purpose of developing powder-based hydrogen storage alloys. Mg and Mg–Ti powder compacts were encapsulated in a copper block and were subjected to ECAP deformation to an apparent strain of $\varepsilon = 4$. This resulted in the consolidation of the compacts as well as in the refinement of their structures. The values of coherently diffracting volume size were as small as 70–80 nm, quite comparable to those achieved with mechanical milling. It is, therefore, concluded that ECAP processing can be employed successfully for the purpose of structural refinement. As for material synthesis, however, the ECAP is less efficient in expanding the interfacial area. Therefore, it is necessary to impose relatively heavy strains to able to achieve comparable expansion in the interfacial area. It appears that an advantage of ECAP deformation is the development of structures which have improved ability for milling. It is, therefore, recommended that in the processing of hydrogen storage alloys, the powder mixtures may be first processed with ECAP in open atmosphere and then by mechanical milling of a short duration carried out under protective atmosphere.

Introduction

A number of routes are available for structural refinement of metallic materials, e.g. mechanical milling [1], repetitive rolling [2], equal channel angular pressing (ECAP) [3], etc. Of these, mechanical milling is a well established method, used widely for the processing of metallic powders. The method not only induces severe plastic deformation but also, quite often, leads to particle fragmentation. In fact the milling with its associated structural refinement has established itself as an efficient method of material synthesis for hydrogen storage alloys [e.g. 4, 5].

Although the effectiveness of mechanical milling is well established in the processing of hydrogen storage alloys especially in intermetallics or intermetallic forming mixtures, it is often very difficult to employ this in ductile powders [6]. Mg and Mg-based powders are not brittle enough and therefore, as illustrated by Çakmak et al. [7], they agglomerate during milling with the resultant increase in particle size. The role of additives is then to help make material brittle so that the milling may lead to particle fragmentation rather than agglomeration. Still, the milling of Mg or Mg-based powders to small particulate sizes is an extremely difficult task [8].

A drawback in the synthesis of hydrogen storage alloys is the difficulty of processing and handling of the powders. As pointed out by Wieczorek et al. [9], there is always a risk of impurity pick-up from the vial and the grinding balls which may alter the chemical make-up of the particulate material. Another drawback is the necessity to process the material under a protective atmosphere. Exposure of powders during or after milling to atmospheres containing O_2, H_2O, etc. are lethal and must therefore be avoided [e.g. 10]. Thus, the powders are often processed and handled under argon atmosphere of high purity, i.e. in a glove box. The problem is aggravated by the fact the milling, when successful, leads to a rapid generation of new surfaces, so the environment to which they are exposed to is of paramount importance.

Clearly an alternative method of material synthesis which would not require a protective atmosphere would be

G. Çakmak · T. Öztürk (✉)
Department of Metallurgical and Materials Engineering,
Middle East Technical University, 06531 Ankara, Turkey
e-mail: ozturk@metu.edu.tr

extremely beneficial. In this respect, ECAP processing appears to be the obvious candidate since the new surfaces generated in this process are negligibly small. The process normally involves a material in bulk form extruded through a die with two channels of equal cross section, intersecting at an angle. The passage of material through the channels produces a simple shear deformation. This method, first used in 1972 by Segal [3], has since been developed in a number of respects; see Valiev and Langdon [11]. Though various forms of ECAP are available, the essence of the process is still the same, i.e. the cross section of the material does not change during the passage, and so the process may be repeated many times enabling the accumulation of extremely large strains. It has been shown for many bulk metallic systems that the ECAP processing leads to drastic structural refinements often leading to the formation of submicron or nanoscale structures [e.g. 12–14].

ECAP has already been employed in the processing of Mg-based hydrogen storage alloys [14–20]. Skripnyuk and co-workers [15] as well as Loken et al. [18] used Mg-rich commercial alloys, or alloys based on Mg–Ni, and following severe plastic deformation examined their hydrogenation behaviour. The processing was carried out in bulk form, i.e. samples from cast alloys were subjected to ECAP deformation.

This study, due to limited compositions which can be cast, concentrates on materials in particulate form. The aim is to explore as to what extent ECAP could be employed, in place of mechanical milling, as a method of both the material synthesis and the structural refinement, this in an effort to develop a cost-effective processing route for hydrogen storage alloys.

Material and method

Elemental powders used in this study were Mg and Ti, each 99.5 wt% pure with −325 mesh size. Samples were prepared from pure Mg and Mg–10 vol.% Ti powders. Two sets of samples were prepared for each; one was processed with ECAP and the other with mechanical milling.

For ECAP processing, the powder was first Spex milled for 10 min and then compacted with a pressure of 200 MPa into 8 mm diameter pellets. For ease of handling, the compacted powders were encapsulated in a copper block. The block was either square in its cross section 14 × 14 mm, or round with 18 mm diameter. This was achieved by drilling a hole of 8 mm diameter from one end. Four pellets, each approximately 20 mm in length, were fitted into the hole. The block was then closed by pressing a copper insert into it. The block was 130 mm in length, so approximately 25 mm at each end was solid copper.

Equal channel angular pressing was carried out by feeding the copper block into a special die. Two die geometries were employed. One was a single zone 90° die that enabled batch processing, and the other was a two-zone 120° die that allowed continuous deformation, Fig. 1.

A single zone die had two identical channels with 14 × 14 mm cross section intersecting at an angle of $\phi = 90°$. The inner corner of the intersection was kept sharp while the outer corner was rounded with $\psi = 20°$, Fig. 1a. Samples were deformed by feeding the copper block into die cavity and pressing the punch onto the block. To eliminate seizure, the punch was forced into the channel, typically by 25 mm, and then removed. A deformable insert was placed into the channel and the operation was repeated in the same manner as before. This continued until the block was forced through the deformation zone and came out from the exit end of the channel. For the geometry in question, i.e. $\phi = 90°$ and $\psi = 20°$, the passage through the deformation zone, imposes a true strain of $\varepsilon = 1.00$ [21]. After the passage, the copper block was re-fed to the die by rotating the sample 90°, i.e. the so-called B_c route, see ref [22].

Two-zone die had circular cross section. The channel angle was 120° in both zones arranged in such a manner that the entry and exit channel was parallel to each other, Fig. 1b. This parallel geometry was adapted from that of Raab [23]. Each zone, in this die, could impose a strain of $\varepsilon = 0.60$ giving a total value of $\varepsilon = 1.2$. The process was automated, i.e. sample was pushed backward and forward in the die a number of times, until the desired level of strain was achieved. The advantage of this parallel die was that it allowed the application of back pressure on opposing punch so that deformation can be carried out with high hydrostatic pressure.

Mechanical milling of ECAPed samples as well as of the initial powders was carried out with a planetary ball mill using 5 mm diameter balls. Due to limited amount of ECAP samples, milling was carried out with a ball-to-powder ratio of 20:1. 1 wt% graphite was added to the powder mixture as anti-sticking agent. Wherever necessary, the particle size is measured with laser scattering using ethanol as dispersant.

Density of the powder compacts were measured by Archimedes principle. Since Mg reacts with water, ethanol was used for volume measurement. Microstructural characterization was carried out using a field emission SEM. Structural refinement in samples was measured in terms of the size of coherently diffracting volumes. For this purpose, X-ray diffractograms were measured in a step scanning mode (0.02° for 3 s) $10° < 2\theta < 90°$ using CuKα radiation (typically 40 kV, 40 mA). Standard Si sample was run at each session of X-ray measurements so as to correct angular shift that might occur in peak positions.

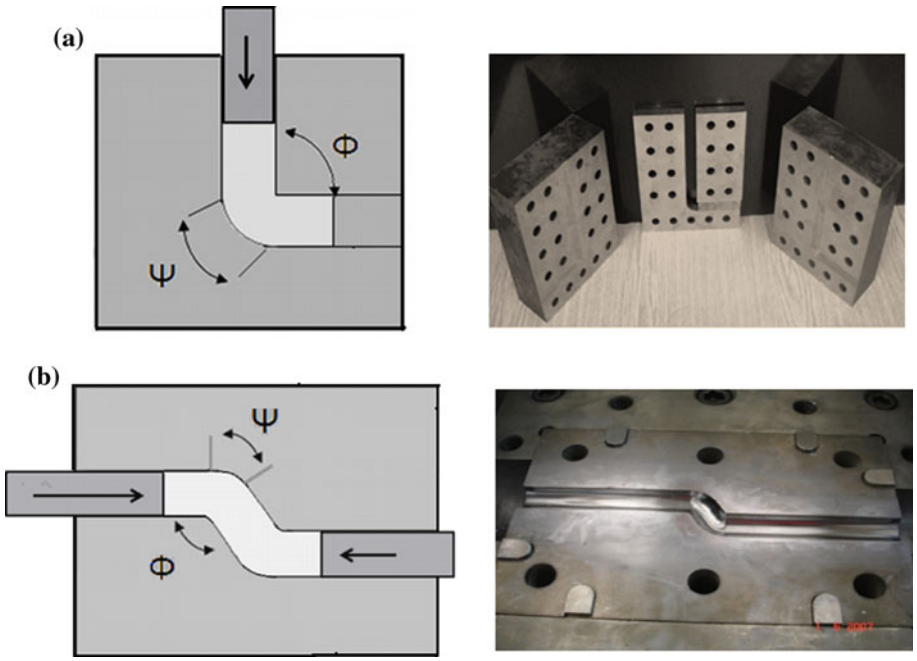

Fig. 1 Dies used for equal channel angular pressing of compacted powder samples. ϕ refers to channel angle, Ψ refers to the angle of curvature. **a** Single zone die with $\phi = 90°$, **b** Two-zone parallel die with $\phi = 120°$. The sample (*white*) is shown in a partially deformed state

The crystallite size, the lattice parameters as well as volume fractions were obtained from the Rietveld refinement of X-ray data.

Results

ECAP processing of Mg and Mg–Ti

The regime of ECAP deformation employed in this study normally involved a single zone die with passage of samples 1, 2, 3 and finally 4 times. This corresponds to true strain values of $\varepsilon = 1, 2, 3$ and 4. Figure 2 shows a typical diffractograms recorded from a Mg sample deformed to $\varepsilon = 4$. Structural parameters derived from X-ray data for Mg and Mg–Ti are given in Tables 1 and 2, respectively. Crystallite size, reported in this table, shows that he powders have been strained as a result of ECAP deformation. The values are such that there is a monotonic decrease with increasing level of strain, both for Mg and Mg–Ti. The size which is initially in the order of 140 nm for Mg decreases to a value of 80 nm after the fourth pass, i.e. a true strain of $\varepsilon = 4.0$. This decrease in the size of the coherently diffracting volumes is also true for Mg–Ti, Mg is reduced down to 70 nm and Ti had a size of 40 nm at the end of fourth pass.

Tables 1 and 2 also contain data from mechanically milled powders. The crystallite sizes of Mg and Mg–Ti, determined after 5 h of milling, are 80 and 70 nm in the respective order. Thus, in terms of coherently diffracting volumes, i.e. crystallite size, both ECAP deformation and mechanical milling leads to similar sizes. It can, therefore, be concluded that ECAP deformation is as efficient as mechanical milling in terms of size reduction in coherently diffracting volumes.

It should be pointed out that the crystallite sizes reported above are not unlike those reported for ECAP deformed solid samples [24, 25]. For instance, Mathis et al. [25] has deformed cast AZ91 alloy (Mg–9 wt% Al) with a 90° die and found a crystallite size of approx. 60 nm after a total strain of $\varepsilon = 9.2$, i.e. 8 passes. To check this, a fully dense Mg sample was prepared from the current Mg powders. The sample hot compacted under 200 MPa at 350 °C for 3 h was subjected to 4 passes using the single zone die. The sample has yielded a crystallite size of 83 nm, which is quite close to the value obtained with the powder compacts (77 nm).

The fact that both powder compact and the fully dense sample yield essentially similar crystallite sizes imply that in ECAP, the powders even when loosely packed respond to the shape change by plastic deformation rather than being re-accommodated as rigid particles. The latter is a possibility since loose powders could flow through the deformation zone simply by translation and rotation without being subjected to plastic deformation. Figure 3 shows a powder compact that has been removed from the Cu block after the first pass. The piece appears to be quite solid with visible shear markings on its surface. Thus, the powder compact seems to have been consolidated as a result of ECAP deformation.

Samples following ECAP deformation were subjected to density measurement so as to establish the level of particle consolidation. The values measured after each pass are shown plotted in Fig. 4. Here the compact which initially

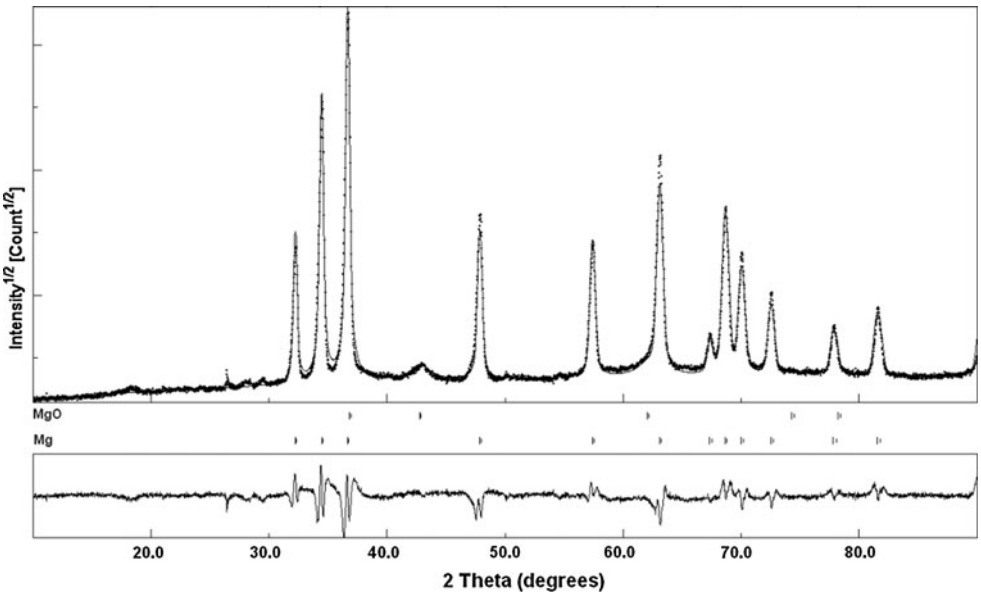

Fig. 2 X-ray diffractogram (Rietveld refined) of Mg ECAP deformed to a true strain of $\varepsilon = 4.0$

Table 1 Structural characteristics of Mg powder compacts ECAP deformed to true strains of $\varepsilon = 1, 2, 3$ and 4

		ECAP deformation (ε)					Powder
		0	1	2	3	4	5 h
Crystallite size (nm)	Mg	138.8 ± 4.2	118.8 ± 5.3	100.2 ± 4.4	89.6 ± 4.6	77.6 ± 5.0	79.7 ± 5.3
Volume fraction of phases	Mg	98.0	98.6	98.5	98.46	98.5	97.6
	MgO	2.0	1.4	1.4	1.5	1.5	2.4
Lattice parameters (Å)	Mg-a	3.21(6)	3.21(5)	3.21(5)	3.21(4)	3.21(4)	3.21(4)
	Mg-c	5.22(1)	5.21(7)	5.21(6)	5.21(7)	5.21(7)	5.21(7)

The same mixture milled for 5 h are also included for comparison

Table 2 Structural characteristics of Mg–10 vol.% Ti powder compacts ECAP deformed to true strains of $\varepsilon = 1, 2, 3$ and 4

		ECAP deformation (ε)					Powder
		0	1	2	3	4	5 h
Crystallite size (nm)	Mg	140.2 ± 6.8	97.4 ± 6.3	75.5 ± 6.2	72.1 ± 7.3	69.9 ± 6.3	72.0 ± 5.3
	Ti	179.3 ± 7.2	57.6 ± 6.7	56.4 ± 5.7	48.0 ± 6.2	40.4 ± 5.7	70.8 ± 4.3
Volume fraction of phases	Mg	91.1	90.1	90.0	90.1	89.8	90.3
	Ti	8.2	8.4	8.5	8.6	8.9	7.9
	MgO	0.7	1.5	1.5	1.3	1.3	1.8
Lattice parameters (Å)	Mg-a	3.21(2)	3.21(0)	3.21(1)	3.21(2)	3.21(3)	3.21(4)
	Mg-c	5.21(4)	5.21(4)	5.21(3)	5.21(6)	5.21(7)	5.21(6)
	Ti-a	2.95(3)	2.95(2)	2.95(2)	2.95(3)	2.95(4)	2.95(5)
	Ti-c	4.68(7)	4.68(6)	4.68(6)	4.68(8)	4.69(0)	4.68(8)

The same mixture milled for 5 h are also included for comparison

had a density of 1.673 g/cm^3 consolidates to a value of 2.029 g/cm^3 after the first pass. This value increases in subsequent passes reaching a value of 2.073 g/cm^3 after the fourth pass. The value is quite close to the density of the hot compacted sample (2.0997 g/cm^3) shown by the horizontal line in Fig. 4. Consolidation of powder compacts via ECAP deformation is a well known phenomenon that has been previously reported for Mg [26, 27] as well as for the other powder systems [28, 29].

Observations reported above imply that feeding of material in powder form does not significantly modify the nature of ECAP deformation. The powders are sufficiently

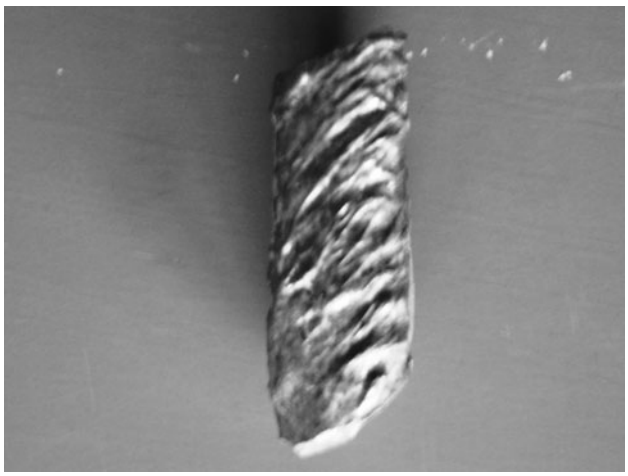

Fig. 3 A Mg powder compact removed from encapsulating copper bar subjected to one pass of ECAP deformation ($\varepsilon = 1$). Note the shear markings on the surface of the sample

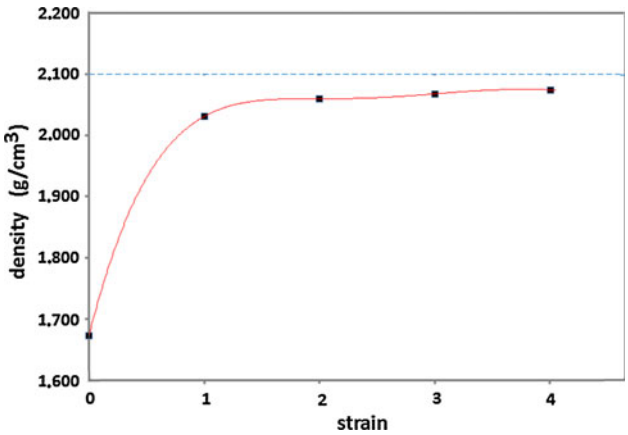

Fig. 4 The variation of density in Mg–10 vol.% Ti with ECAP deformation. Note that the density increase in the first pass is quite high

consolidated even in the first pass so that the process results in the formation of nanosize volumes in much the same way as in the solid samples.

Microstructures in the ECAP processed powder compacts are given in Figs. 5 and 6. Figure 5b refers to a longitudinal section of a pure Mg after the fourth pass. Here grains originating from the powder particles which are initially equiaxed, Fig. 5a, seem to have been inclined at an angle to the shear (longitudinal) direction. Angular distortions of grains are also apparent. Microstructure of the same sample at the transverse section is given in Fig. 5c. It is worth noting that the length scale in Fig. 5c is still comparable to that of Fig. 5a. This is despite the fact that the latter sample was subjected to a very high strain ($\varepsilon = 4$).

Microstructures in Mg–Ti display similar features. Figure 6a and c refer to the transverse section of the sample

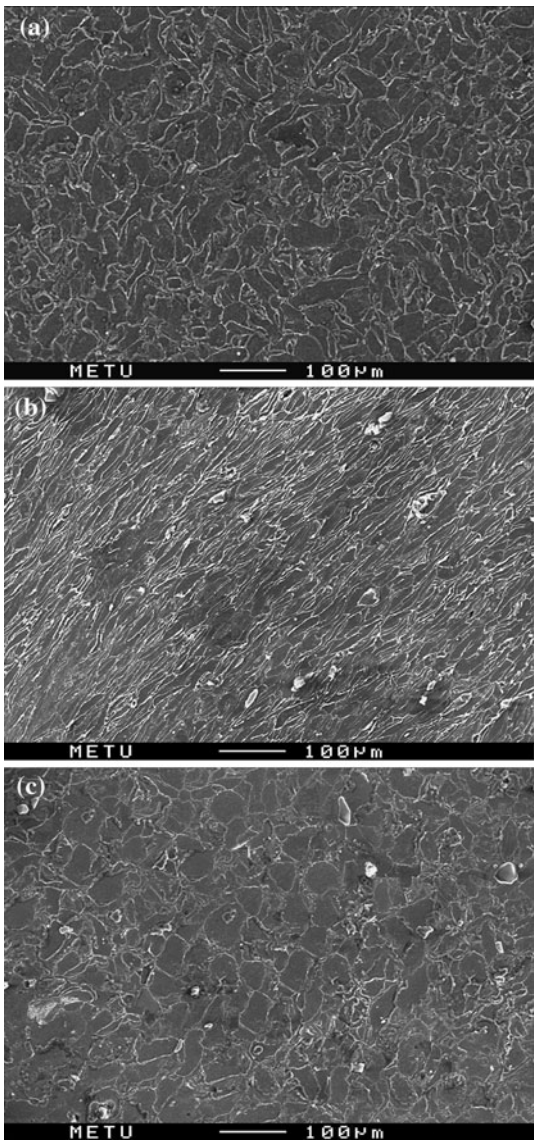

Fig. 5 Microstructures in Mg powder compact. **a** Initial structure (transverse section), **b** and **c** after ECAP deformation $\varepsilon = 4$. **b** refers to longitudinal section; shear plane is the paper plane, shear direction is horizontal and **c** refers to transverse section. Note that the scale of structure in **c** is not too different from that in (**a**)

before and after ECAP deformation. Here, the length scales are again quite comparable to each other, despite the heavy strain imposed. In addition, Ti particles seem to have been deformed less than Mg. This is quite clear in Fig. 6b which shows the longitudinal section of the deformed sample. Here Ti particles seem to have been translated without much sign of distortion. Inset in Fig. 6b shows a locality in this sample where Mg was subjected to a complex flow pattern, presumably to accommodate the Ti particles that remains un-deformed or deformed less.

Particulate structures resulting from milling of Mg are shown in Fig. 7a–e. It should be noted that the milling does not reduce the particle size. The Mg particles seem to have

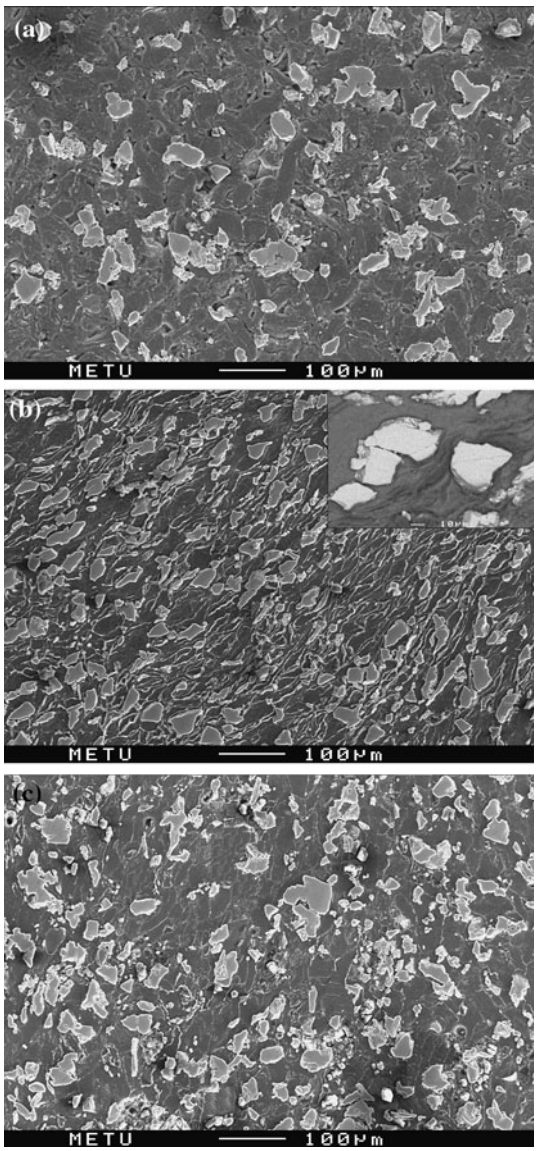

Fig. 6 Microstructures in Mg–10 vol.% Ti powder compact. **a** Initial structure (transverse section), **b** and **c** after ECAP deformation $\varepsilon = 4$. **b** refers to longitudinal section; shear plane is the paper plane, shear direction is horizontal. *Inset* in **b** shows a locality in this section where Mg was subject to a rather complicated flow pattern. **c** refers to transverse section. Note that the scale of structure in **c** is not too different from that in (**a**)

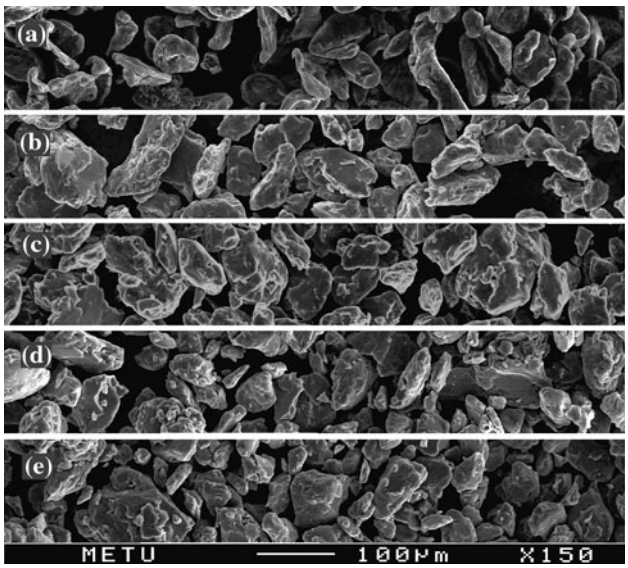

Fig. 7 SEM micrographs of Mg powder after milling for **b** 0.5 h, **c** 1 h, **d** 2 h, **e** 5 h. **a** refers to the starting powder

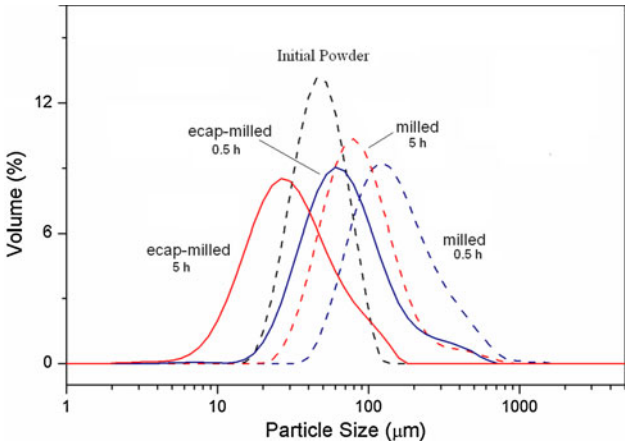

Fig. 8 Particle size distribution of Mg powders obtained after direct milling (*dotted lines*) and milling after ECAP deformation ($e = 4$) (*continuous lines*). Note that ECAP deformed Mg yields finer particles with milling

been agglomerated and have sizes which are in fact larger than the starting powder, Fig. 8. In Mg–Ti, Mg particles behaved in similar manner. Ti particles on the other hand have been refined quite drastically. They appeared as small fragments that have been distributed throughout the particulate structure. The agglomeration of Mg particles in the one hand and the disintegration of Ti particles, on the other, imply that the structure, under the repeated impacts of the balls, is determined by a balance between the fragmentation arising from ductile fracture and agglomeration resulting from the cold welding process. The result of these repeated impacts is that the particulate structure are heavily mixed and refined. This is well illustrated in Fig. 9 where the particulate structure shown refers to Mg–Ti after 1 h of milling. Thus, even when Mg is agglomerated Ti has been refined and distributed uniformly over the structure.

The observations made above show that ECAP processing and mechanical milling differ from each other quite drastically in terms of resulting micro/particulate structure. While in milling, the volume elements are mixed together and re-distributed continuously. This is not the case for ECAP processing. This difference is well reflected in the distribution of Ti constituent in both samples. In Fig. 9, Ti appears as tiny pieces formed as a result of repeated impacts in milling. In Fig. 6c which refers to ECAP

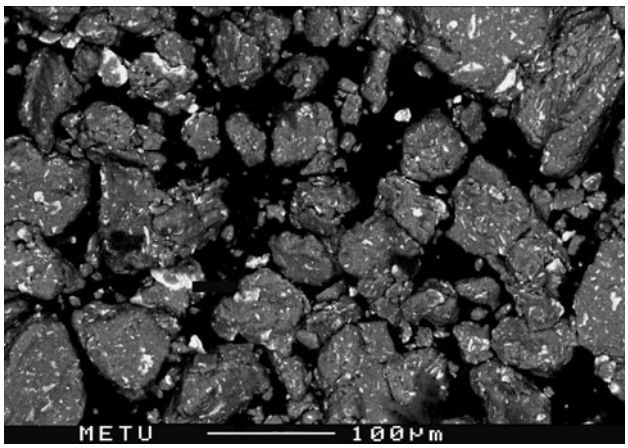

Fig. 9 SEM micrograph of Mg–10 vol.% Ti milled for 1 h. Bright phase is Ti

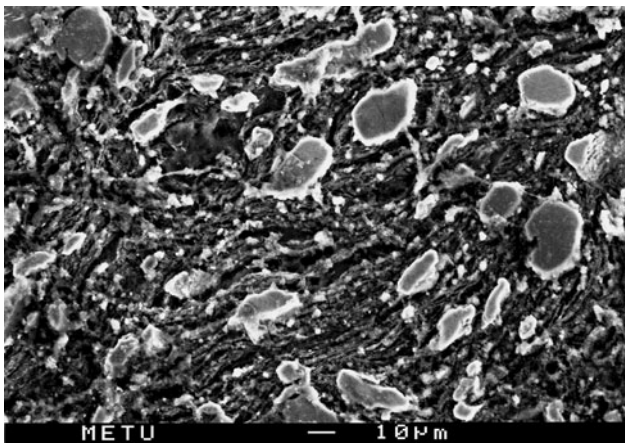

Fig. 10 Microstructure of Mg–Ti deformed to $\varepsilon = 24$ (10 pair of passes) using the parallel die

deformed sample, the phase is very large in comparison and appears in sizes which are only slightly less than the initial particles size, Fig. 6a.

The size reduction achievable with plastic deformation is not necessarily small. This has been well demonstrated in rolling deformation of metal–metal systems [30]. For instance, in Fe–Cu multilayer, Shingu et al. [31] reports a size reduction of 1:100 obtained after a rolling deformation of $\varepsilon = 4$, i.e. final size of 500 nm obtained from 45 μm thick layers. The deformation imposed in this study is quite comparable to the strain imposed in this study.

The preservation of the initial length scale though surprising when contrasted with the more conventional processing techniques is the direct result of simple shear deformation. An important parameter in this respect is the interfacial area, i.e. the rate with which it increases with the imposed strain. A grain or a phase, cubic in shape, for instance when subjected to a true strain of $\varepsilon = 4.0$, i.e. the same strain that was imposed in this study, the interfacial area increases by a factor of roughly 8. The same deformation when imposed in for instance in rolling on the other hand, the area increases by a factor of more than 100. Thus, to reach a similar degree of refinement, much higher strain would be needed in ECAP deformation.

To test this, a Mg–Ti sample was prepared and deformed in parallel ECAP die. A total of ten pair of passes have been imposed which corresponds to a true strain of $\varepsilon = 24$. Figure 10 shows the transverse section of this sample. Here Mg grains seem to have been heavily distorted in a complicated pattern. Ti particles seem to have been refined in a manner as if they have been eroded by Mg flow around them. This erosion is consistent with the presence of tiny Ti fragments as well as rounded shapes of the larger fragments. Thus, the structure obtained after a true strain of $\varepsilon = 24$ is not unlike to that obtained after milling.

The mixing and refinement of structure that takes place with heavy ECAP deformation were also reported in Mg–Mm–Ni [18] and Mg–Ni [16]. In the former study, Loken et al. converted the heterogonous as-cast structure into a fine microstructure via ECAP deformation with a true strain of $\varepsilon = 8$. Moreover Skripnyuk et al. [16] noting the presence of Ni gradient near Mg_2Ni particles implied mixing at much finer scale.

Milling after ECAP deformation

Since hydrogen storage alloys are used in particulate form, it is necessary to covert the consolidated materials resulting from ECAP deformation into a granular form. Figure 11 shows the particulate structures obtained after mechanical milling of ECAP deformed Mg sample. Of these, Fig. 11a refers to structure after 30 min of milling. The average particle size has a value of 71 μm. This value is significantly less than the sizes obtained with direct milling of Mg powders. To

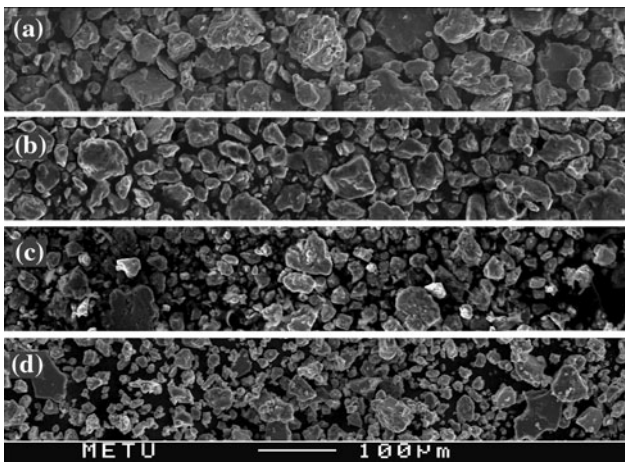

Fig. 11 SEM micrographs of Mg powder compacts ECAP deformed to $\varepsilon = 4$ and milled for **a** 0.5 h, **b** 1 h, **c** 2 h, **d** 5 h

verify this, ECAPed deformed samples were subjected to the milling operations using the same conditions and durations as above. Thus, milling was extended to 5 h, samples being taken after 60 and 120 min. Particle size distribution determined for these samples are included in Fig. 8. It is seen that the size distribution of milled ECAPed samples centres on values which are significantly less than those obtained by direct milling. For instance after 5 h of milling, milled ECAPed sample has $d_v(0.5) = 31$ μm. This should be compared with $d_v(0.5) = 88$ μm obtained with direct milling.

The observation that milling after ECAP deformation leads to more efficient size reduction has probably some relevance to the improved hydrogenation behaviour reported by Skripnyuk et al. [15] and Loken et al. [18]. In these studies, the highest desorption rate was observed when ECAP deformed samples were further processed by milling.

Discussion

The advantage of ECAP processing over mechanical milling is that the particles embedded in the sample, expect those at the very surface, are isolated from the environment in which the processing is carried out. This is of considerable advantage in the processing of hydrogen storage alloys since they are poisoned when exposed to atmospheres that contain O_2, H_2O, etc. Thus, the efficient refinement and mixing of phases achieved in ECAP processing is of considerable advantage implying that ECAP can be employed as a technique of material synthesis.

The fact that ECAP deformed sample has a better milling ability is quite important and provides a new approach in the milling of ductile powders. Ductile powders are difficult to mill due to cold welding of particles which leads to agglomeration, i.e. increase in particle size with milling, rather than particle fragmentation, as was the case above.

Based on the observations reported above, a processing route for ductile powders might involve two steps. In the first step, the powders in loose form could be fed into a die, similar to those depicted in Fig. 1b and subjected to several cycles of ECAP deformation. In the second step, the solid piece removed from the die in strain hardened form may be subjected to mechanical milling of a short duration.

Conclusions

In this study, the possibility of employing ECAP processing in lieu of mechanical milling was explored for the purpose of both structural refinement and material synthesis. Mg and Mg–Ti powder compacts encapsulated in copper were subjected to ECAP deformation. The study has shown that

1. ECAP processing leads to consolidation of powder compacts producing almost fully dense samples. As a result, the particles in the compact deform in much the same way as grains in the bulk material.
2. ECAP processing leads to structural refinement of powder particles resulting in coherently diffracting volume sizes that are comparable to those obtained with mechanical milling.

In this respect, ECAP processing and mechanical milling are quite similar.

3. ECAP processing, however, does not seem to be very efficient in generating or expanding the inter-particle boundaries. Thus, for efficient mixing of phases, required for such purposes as material synthesis, it is necessary to employ extremely high strains.

Finally,

4. For size reduction, it appears that ECAP processing even with several passes may be employed quite usefully for the purpose of the improving the milling ability of the powders.

The last point implies a two step approach in the processing of hydrogen storage alloys. The powder mixtures may be first processed with ECAP in open atmosphere and then by a short duration of mechanical milling carried out under protective atmosphere.

Acknowledgements Support for this study was provided by DPT with project number BAP-03-08-DPT.200305K120920-20 and by the FP6 program of the European Commission project (FP6-200-3-518-271), NESSHY, which we gratefully acknowledge.

References

1. Suryanarayana C (2001) Prog Mater Sci 46:1
2. Pedneault S, Huot J, Roue L (2008) J Power Sour 185:566
3. Segal VM (1999) Mater Sci Eng A 271:322
4. Güvendiren M, Baybörü E, Öztürk T (2004) Int J Hydrogen Energy 29:491
5. Mandzhukova T, Bobet J-L, Khrussanova M, Peshev P (2009) Mater Res Bull 44:1968
6. Huang JY, Wu YK, Ye HQ (1995) Mater Sci Eng A 199:165
7. Çakmak G, Károly Z, Mohai I, Öztürk T, Szépvölgyi J (2010) Int J Hydrogen Energy 35:10412
8. Zaluska A, Zaluski L, Ström–Olsen JO (1999) J Alloy Compd 288:217
9. Wieczorek AK, Krystian M, Zehetbauer MJ (2006) Solid State Phenom 114:177
10. Ivey DG, Northwood DO (1983) J Mater Sci 18:321. doi: 10.1007/BF00560621
11. Valiev RZ, Langdon TG (2006) Prog Mater Sci 51:881

12. Komura S, Horita Z, Nemoto M, Langdon TG (1999) J Mat Res 14:4044
13. Pushin VG, Stolyarov VV, Valiev RZ, Kourov NI, Kuranova NN, Prokofiev EA, Yurchenko LI (2002) Ann Chim Sci Mater 27:77
14. Zehetbauer M, Grössinger R, Krenn H, Krystian M, Pippan R, Rogl P, Waitz T, Würschum R (2010) Adv Eng Mater 12:692
15. Skripnyuk VM, Rabkin E, Estrin Y, Lapovok R (2004) Acta Mater 52:405
16. Skripnyuk V, Buchman E, Rabkin E, Estrin Y, Popov M, Jorgensen S (2007) J Alloy Compd 436:99
17. Çakmak G, Bobet J-L, Ölmez R, Öztürk T (2007) In: Proceedings International Hydrogen Energy Congress and Exhibition IHEC, Istanbul, Turkey
18. Loken S, Solberg JK, Maehlen JP, Denys RV, Lototsky MV, Tarasov BP, Yartys VA (2007) J Alloy Compd 446–447:114
19. Sprinyuk VM, Rabkin E, Estrin Y, Lapovok R (2009) Int J Hydrogen Energy 34:6320
20. Leiva DR, Fruchart D, Bacia M, Girard G, Skryabina N, Villela ACS, Miraglia S, Santos DS, Botta WJ (2009) Int J Mater Res 100:1739
21. Iwahashi Y, Wang J, Horita Z, Nemoto M, Langdon TG (1996) Scr Mater 35:143
22. Furukawa M, Iwahashi Y, Horita Z, Nemoto M, Langdon TG (1998) Mater Sci Eng A 257:328
23. Raab GI (2005) Mater Sci Eng A 410–411:230
24. Dinkel M, Pyczak F, May J, Höppel HW, Göken M (2008) J Mater Sci 43:7481. doi:10.1007/s10853-008-2859-8
25. Máthis K, Gubicza J, Nam NH (2005) J Alloy Compd 394:194
26. Wu HM, Hung SS, Lee PY (2007) J Alloy Compd 434–435:386
27. Moss M, Lapovok R, Bettles CJ (2007) JOM 59:54
28. Xia K, Wu X (2005) Scr Mater 53:1225
29. Quang P, Jeong YG, Yoon SC, Hong SH, Kim HS (2007) J Mater Process Technol 187–188:318
30. Öztürk T, Mirmesdagh J, Ediz T (1994) Mater Sci Eng A 175:125
31. Shingu PH, Ishihara KN, Otsuki A, Daigo I (2001) Mater Sci Eng A 304–306:399